Supplementary Information

Light-triggered strand exchange reaction using the change in the hydrogen bonding pattern of a nucleobase analogue

Kunihiko Morihiro, Tetsuya Kodama, Reiko Waki and Satoshi Obika*

Graduate School of Pharmaceutical Sciences, Osaka University

1-6 Yamadaoka, Suita, Osaka 565-0871 Japan

obika@phs.osaka-u.ac.jp

1. ^{1}H, ^{13}C and ^{31}P spectra of new compounds

1-1. ^{1}H spectrum of compound 2

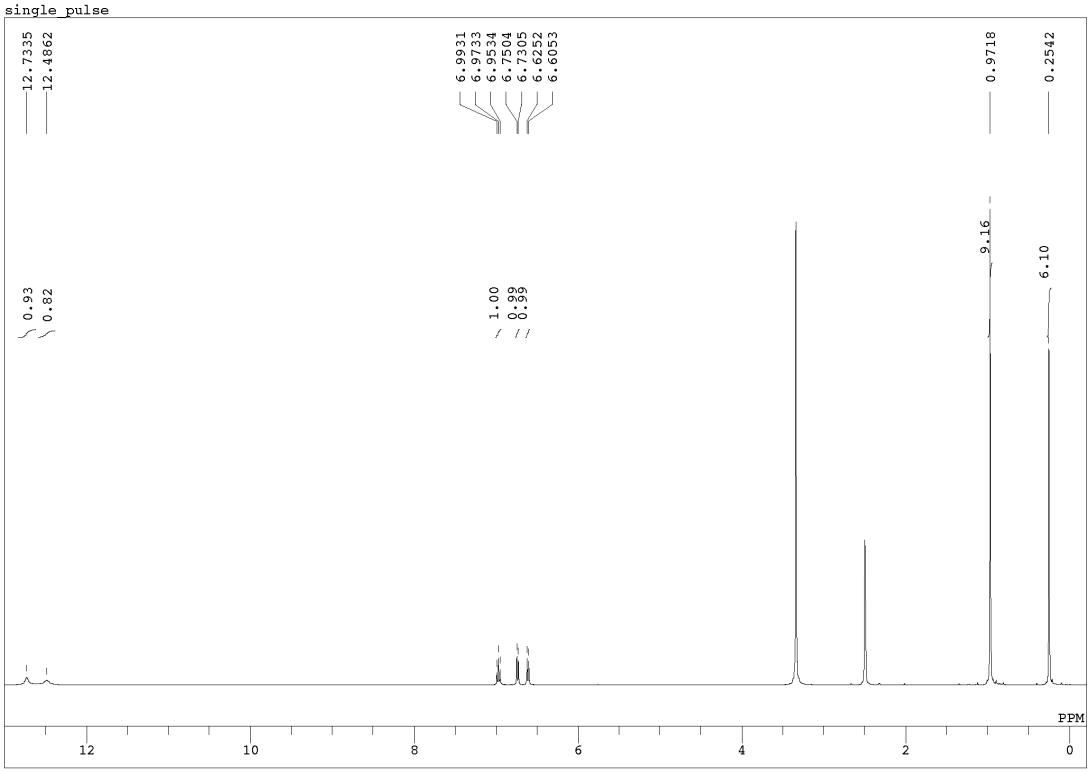

1-2. ^{13}C spectrum of compound 2

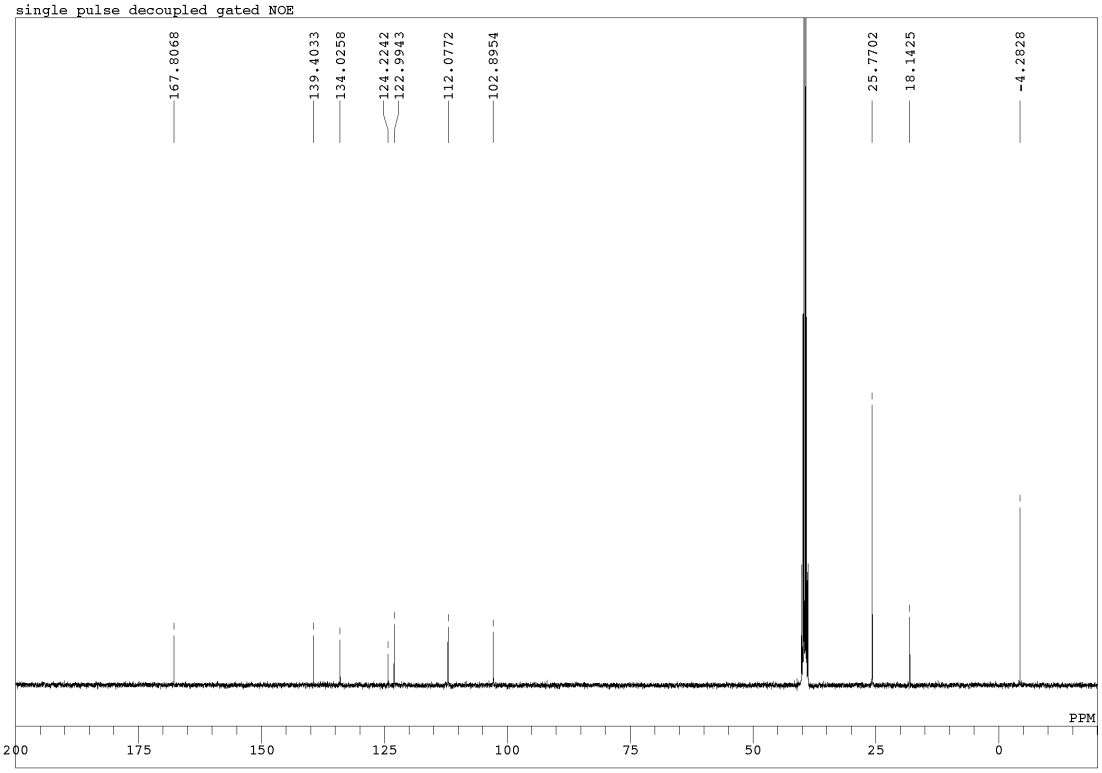

1-3. ^{1}H spectrum of compound 4

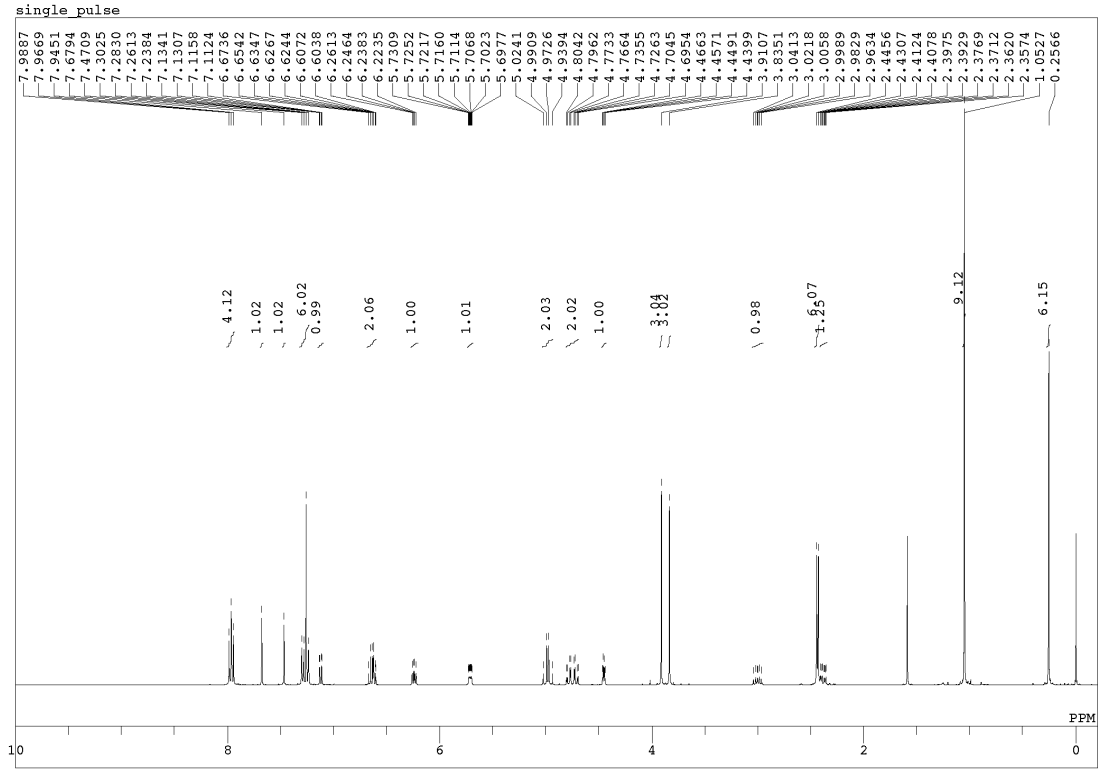

1-4. ^{13}C spectrum of compound 4

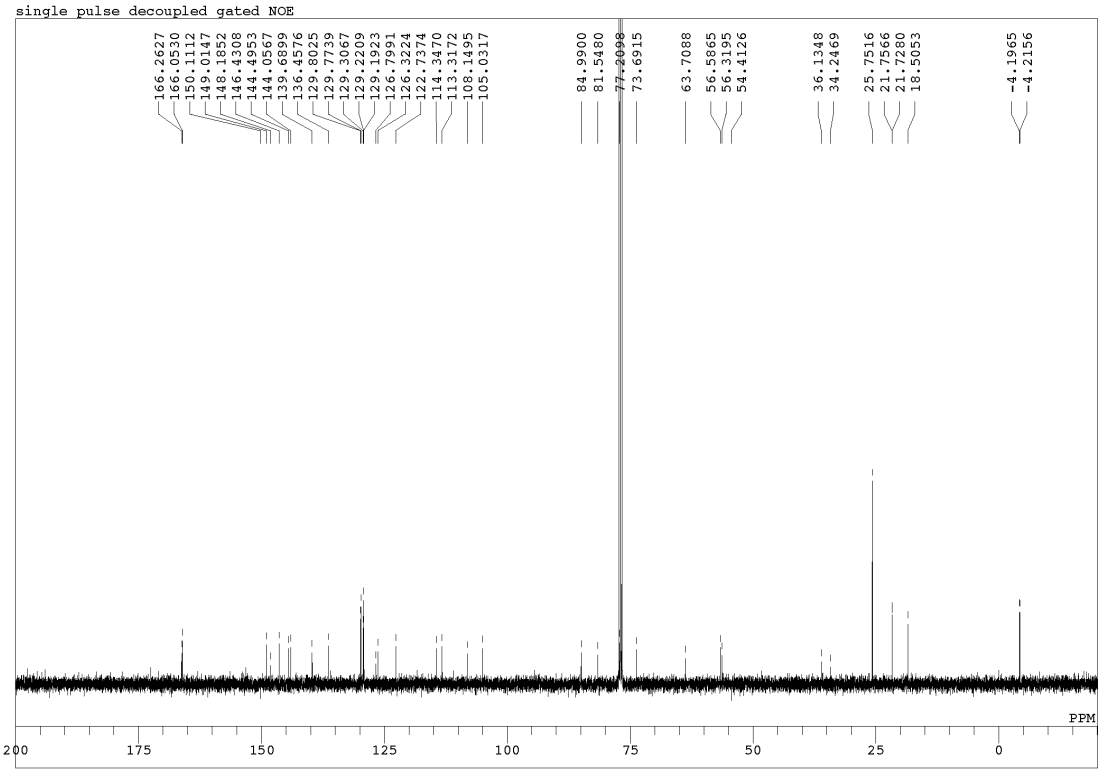

1-5. ^{1}H spectrum of compound 5

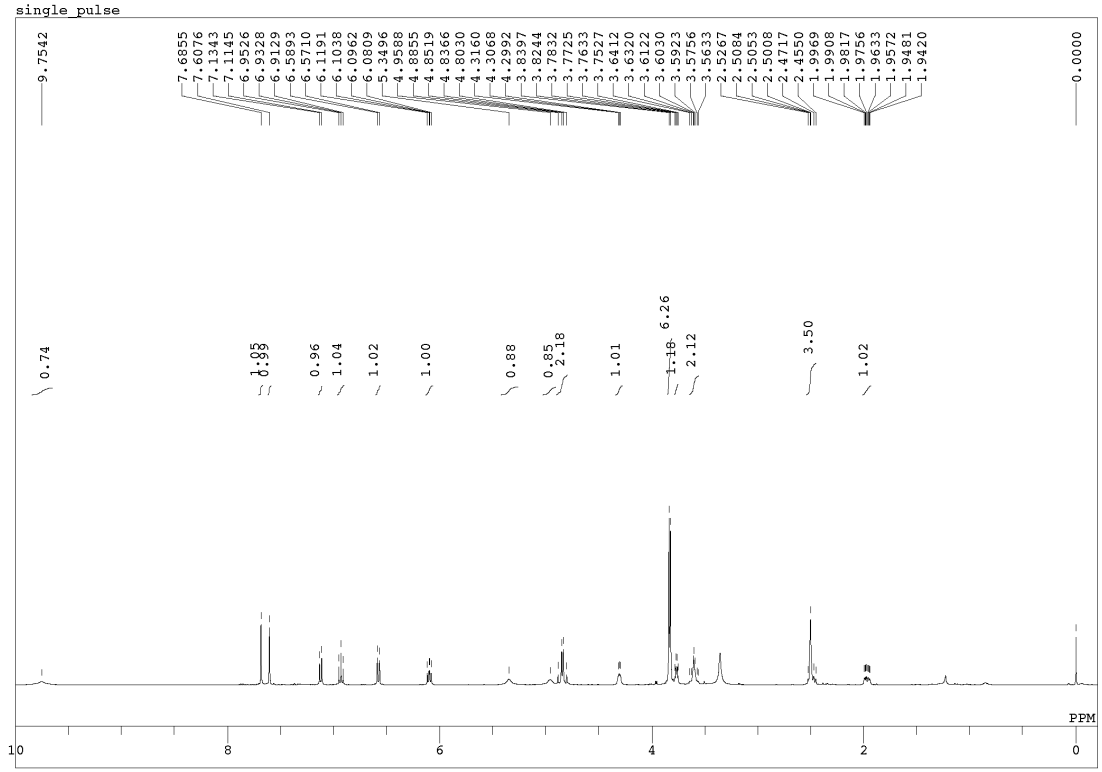

1-6. ^{13}C spectrum of compound 5

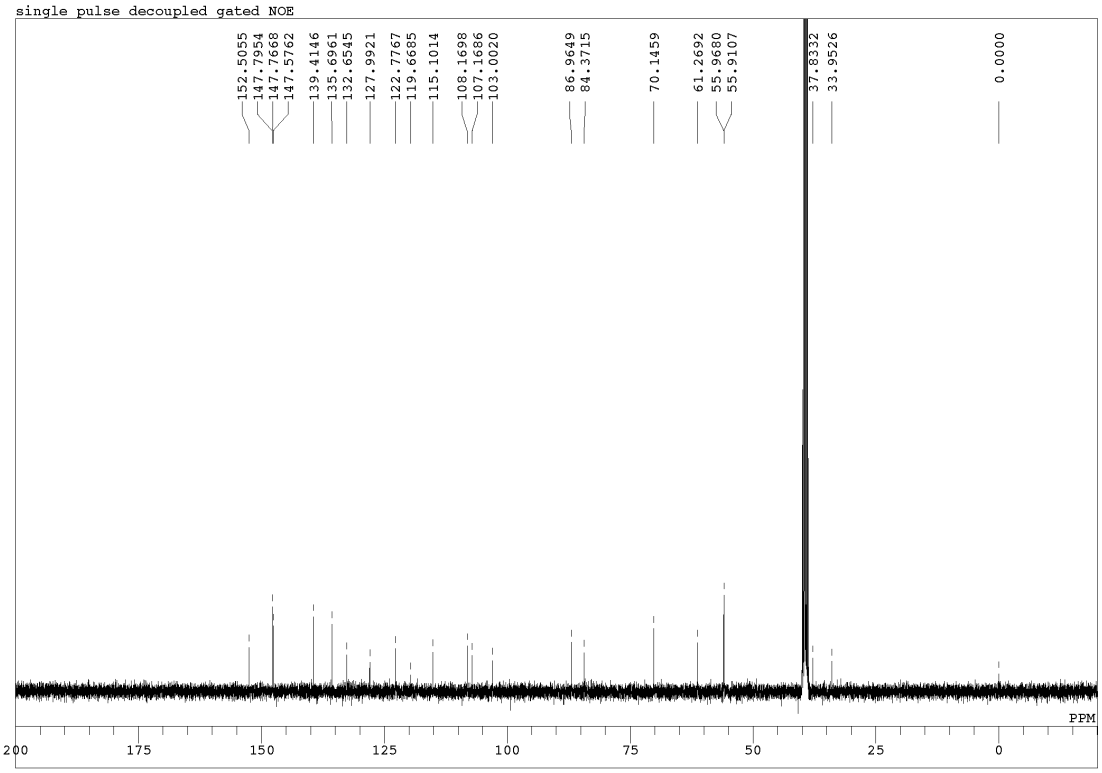

1-7. ^{1}H spectrum of compound 6

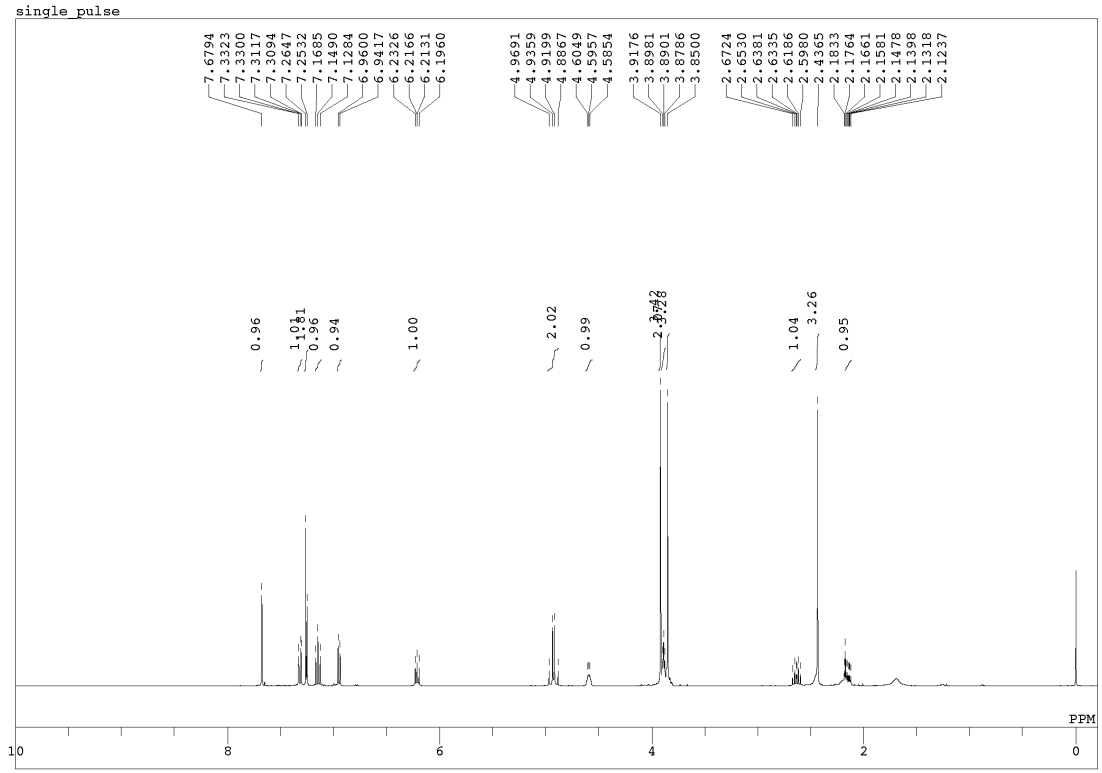

1-8. ^{13}C spectrum of compound 6

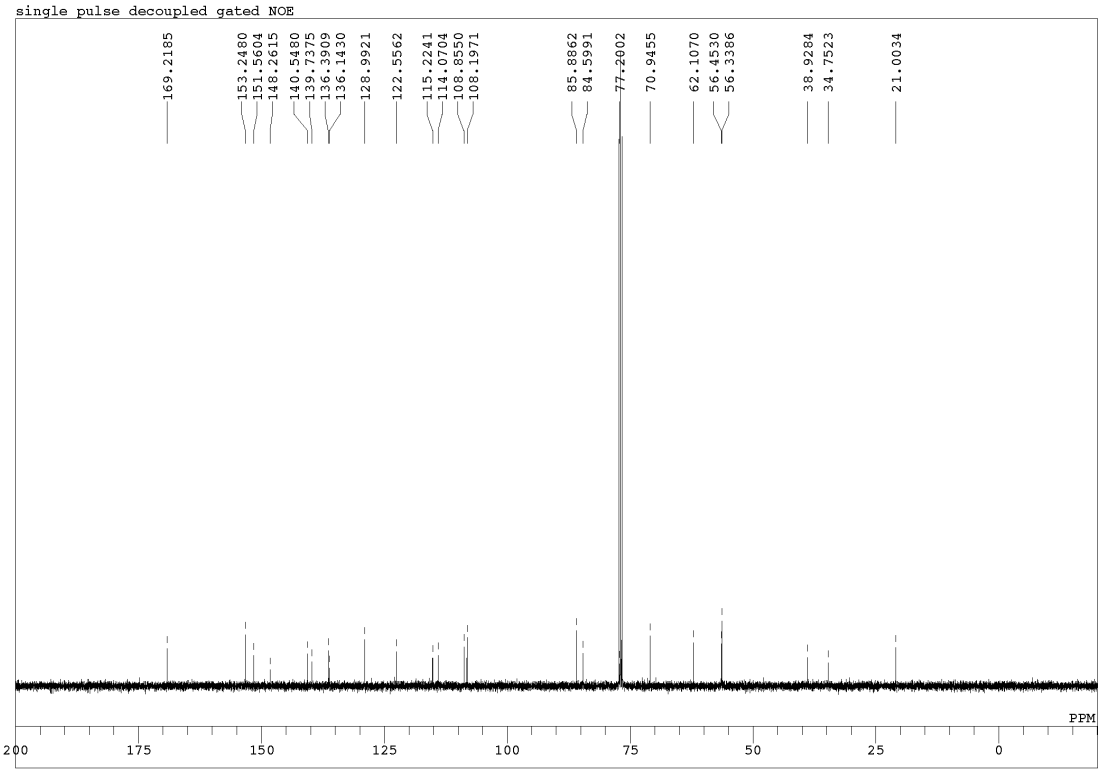

1-9. ^{1}H spectrum of compound 7

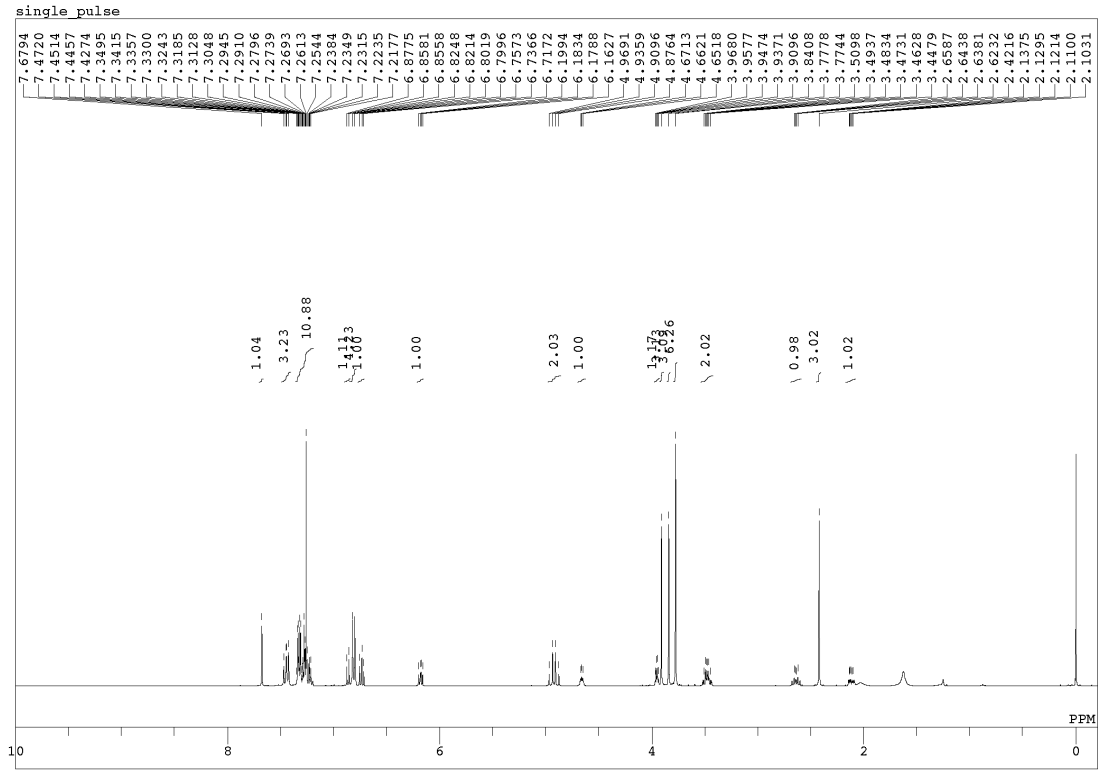

1-10. ^{13}C spectrum of compound 7

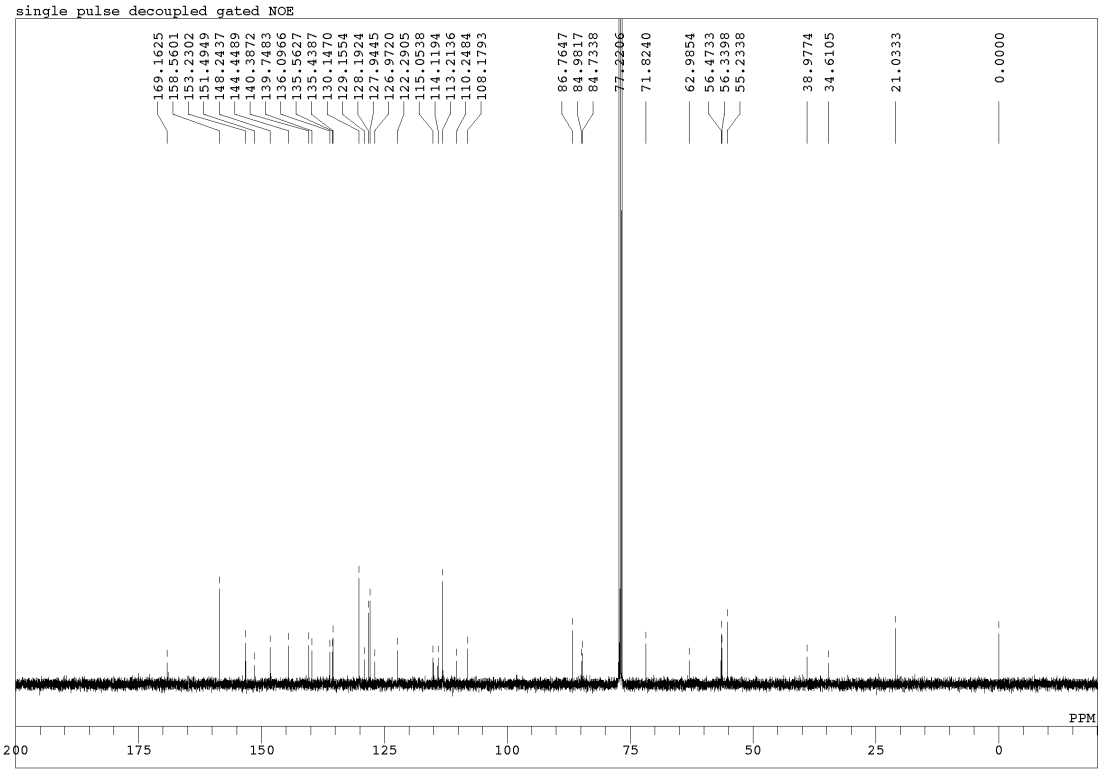

1-11. ^{1}H spectrum of compound 8

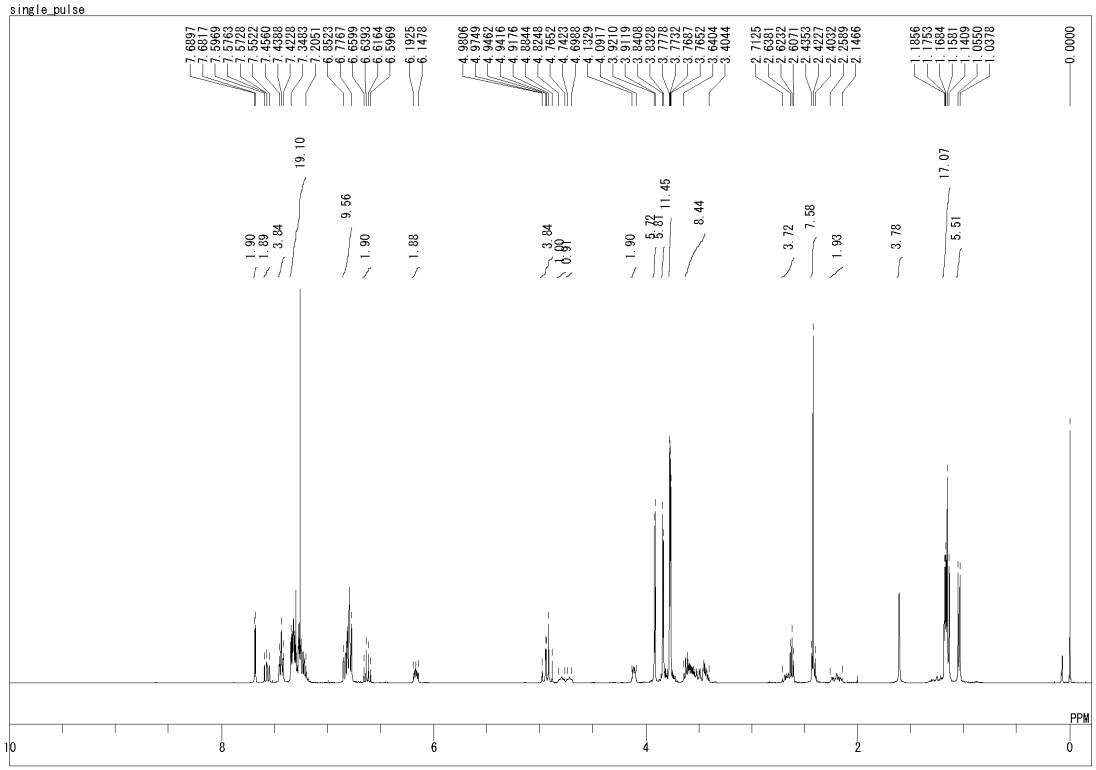

1-12. ^{13}C spectrum of compound 8

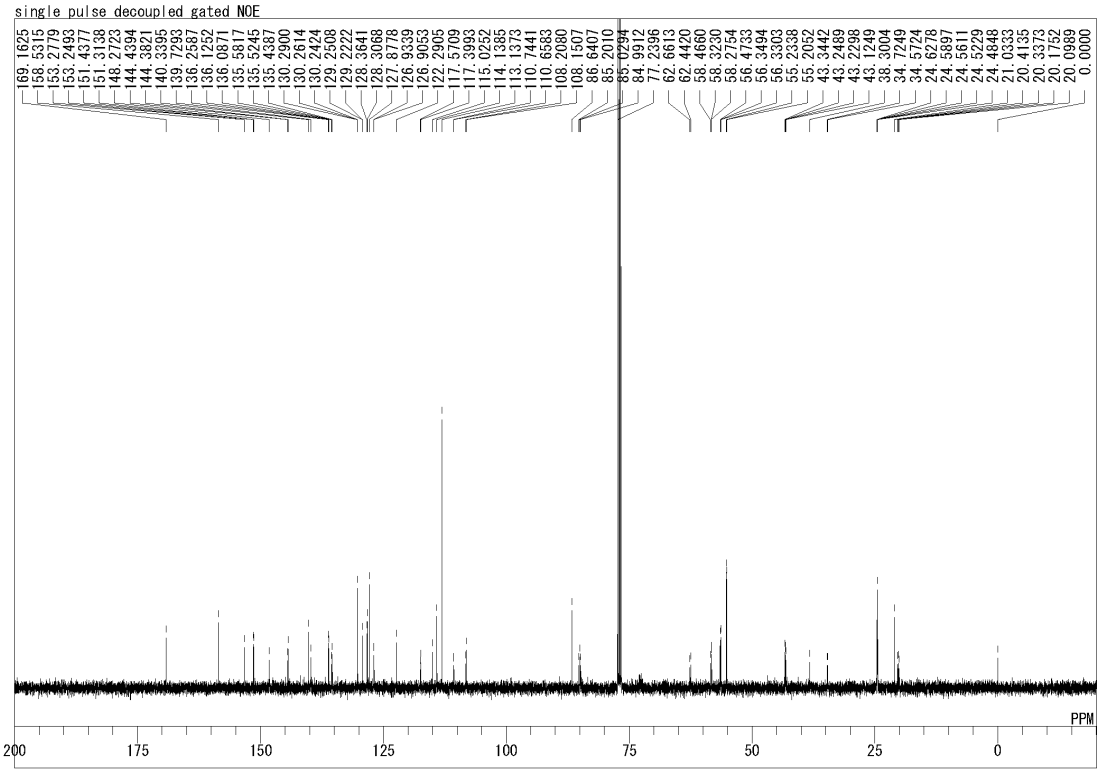

1-13. ^{31}P spectrum of compound 8

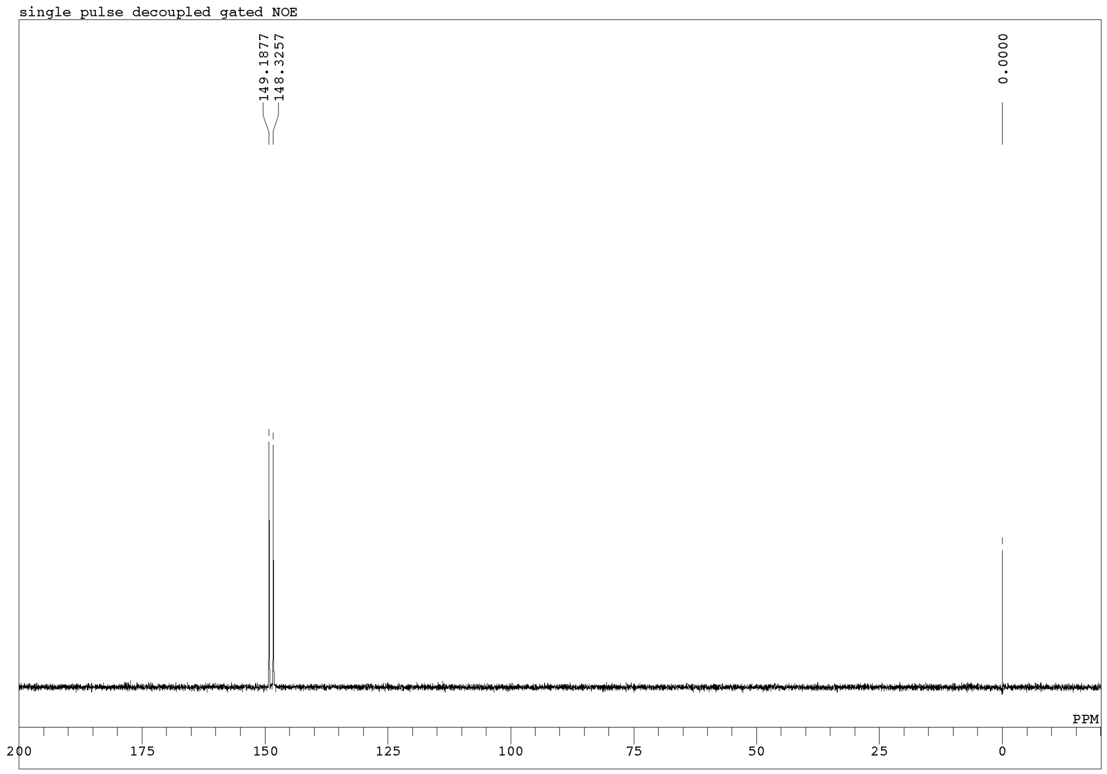

2. Molecular modeling for base pairing

Molecular modeling for base-pairing was performed by consecutive molecular mechanics and molecular orbital calculations with Mac Spartan 10' (Wavefunction Inc.). First, a double strand DNA (dsDNA) containing **SB**$^{\mathbf{NV}}$ was build as a B-type helix using conditions during which only **SB**$^{\mathbf{NV}}$-nucleotides atoms could move. Next, every structure generated randomly by rotating every torsion angles concerning **SB**$^{\mathbf{NV}}$-nucleotide were optimized under MMFF (aq) force field, which was carried out with the end base-pairings constrained. Finally, every **SB**$^{\mathbf{NV}}$-base moiety extracted from the optimized structure was further optimized under HF/6-31G* level. Pictures were drawn with PyMol ver.0.99.

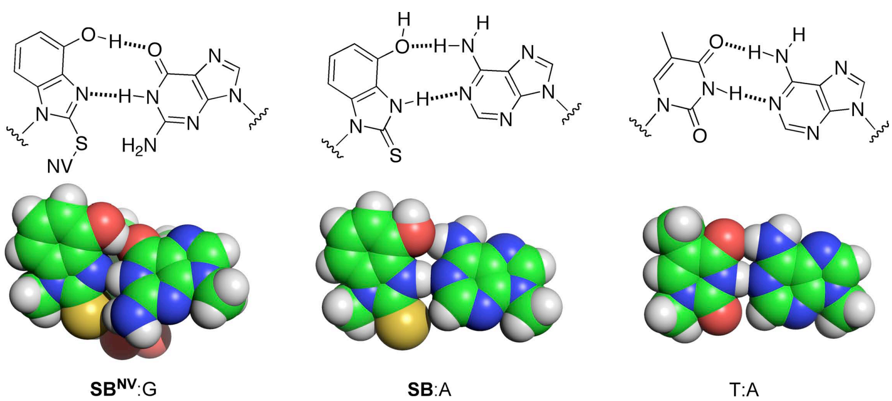

Fig. S1. Comparison of **SB**$^{\mathbf{NV}}$:G, **SB**:A and natural T:A pair as space filling models.

3. HPLC and MALDI-TOF MS analysis of SB^{NV}-modified ODNs

3-1. ODN1

RP-HPLC

Column: Waters XBridge™ OST C18 2.5 μm, 4.6 x 50 mm

Gradient: 6-15% MeCN (over 15 min) in triethylammonium acetate buffer (pH 7.0, 0.1 M)

Flow rate: 1.0 mL/min

Column temperature: 50 ˚C

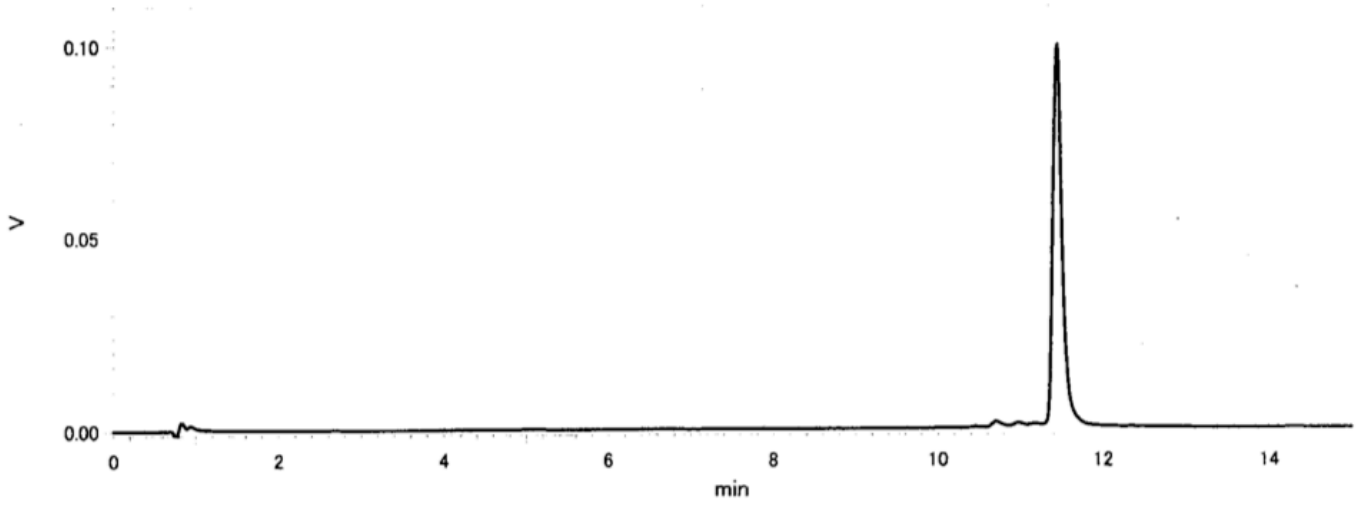

MALDI-TOF MS

Calcd. 3881.7 $[M-H]^-$

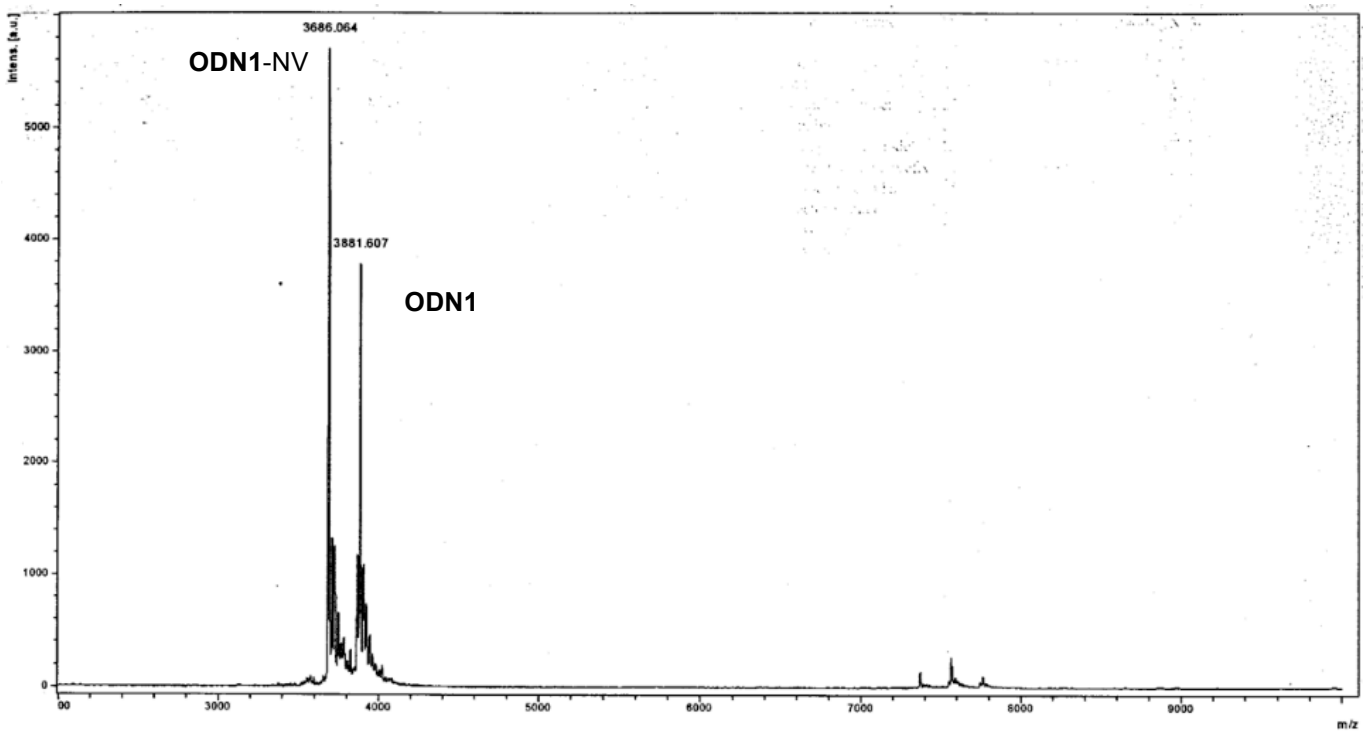

3-2. ODN2

RP-HPLC

Column: Waters XBridge^{TM} OST C18 2.5 μm, 4.6 x 50 mm

Gradient: 6-15% MeCN (over 15 min) in triethylammonium acetate buffer (pH 7.0, 0.1 M)

Flow rate: 1.0 mL/min

Column temperature: 50 ˚C

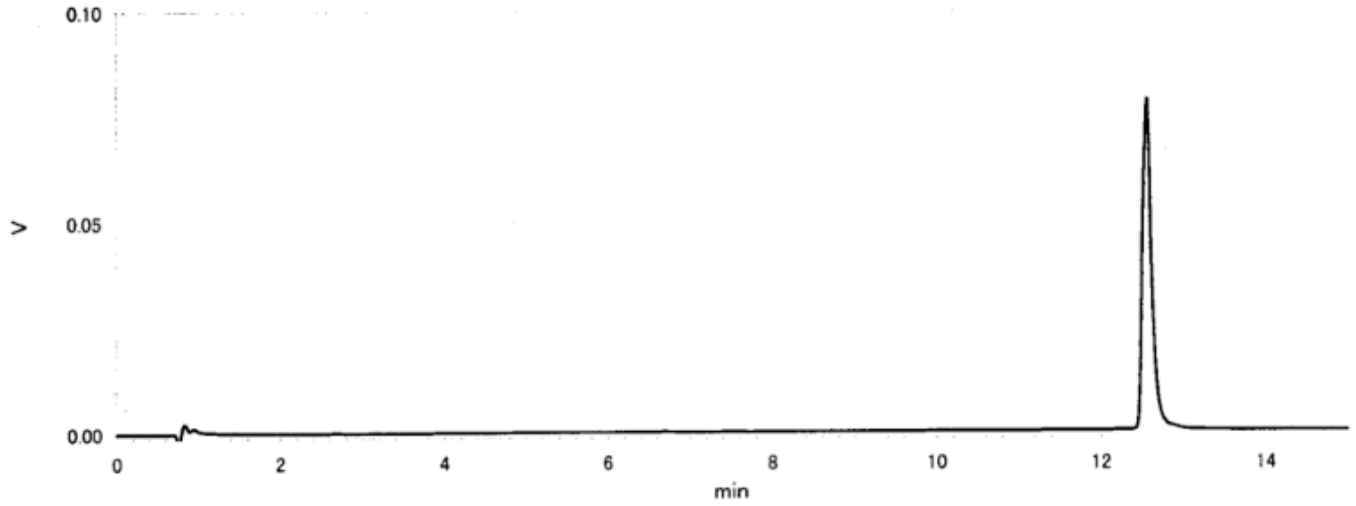

MALDI-TOF MS

Calcd. 3867.6 $[M-H]^-$

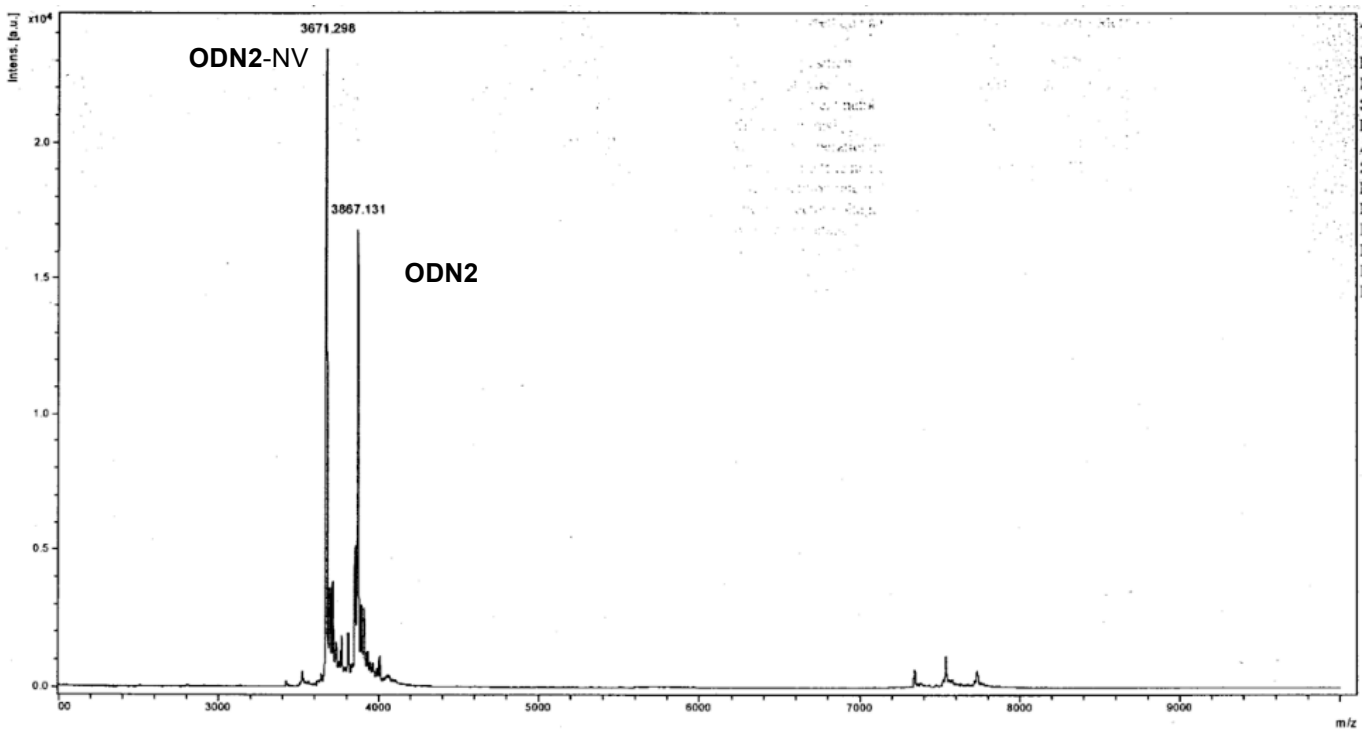

3-3. ODN3

RP-HPLC

Column: Waters XBridge^{TM} OST C18 2.5 μm, 4.6 x 50 mm

Gradient: 8-24% MeCN (over 15 min) in triethylammonium acetate buffer (pH 7.0, 0.1 M)

Flow rate: 1.0 mL/min

Column temperature: 50 ˚C

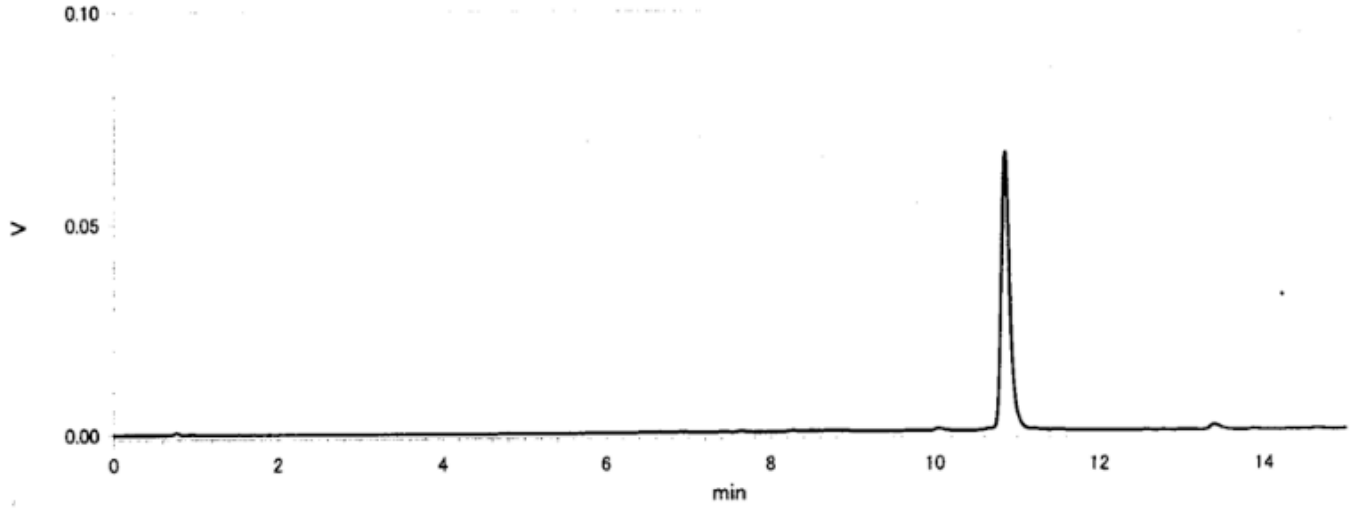

MALDI-TOF MS

Calcd. 3737.7 $[M-H]^-$

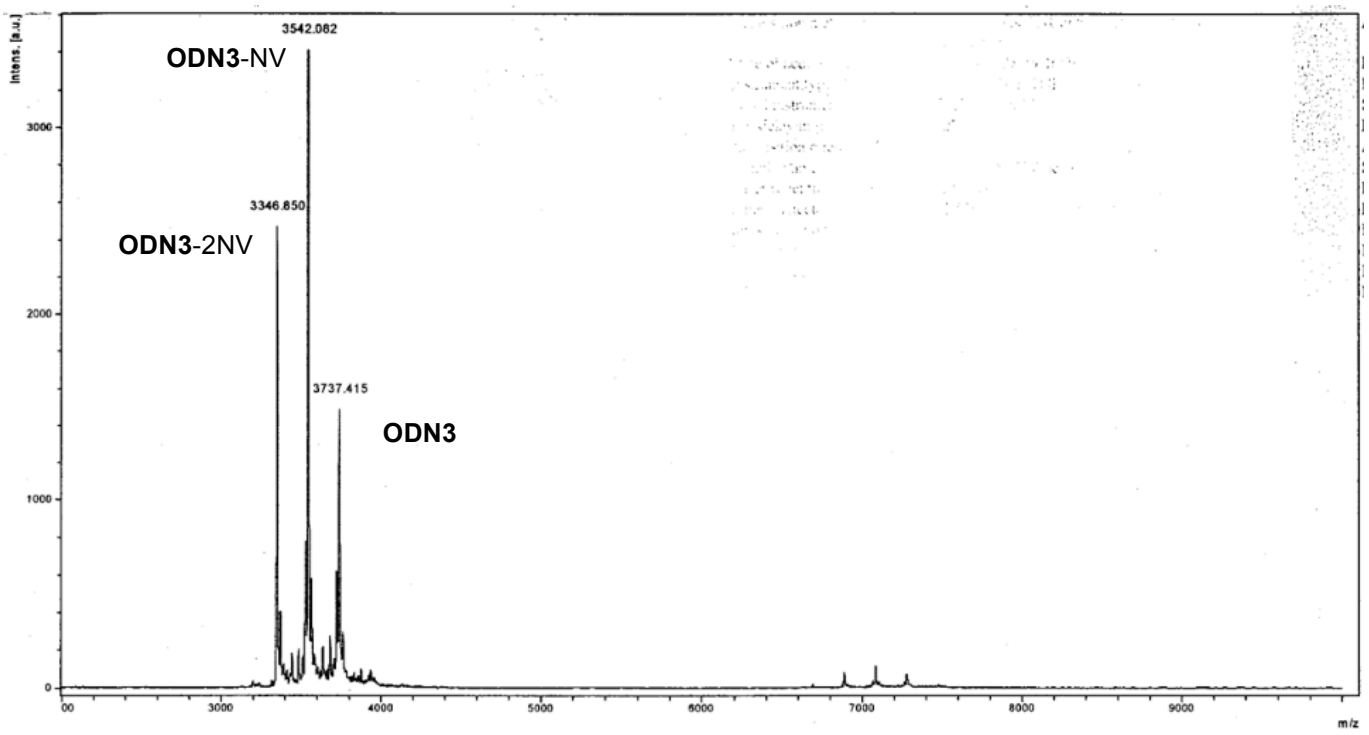

4. Photoreaction of SB^{NV}-modified ODNs

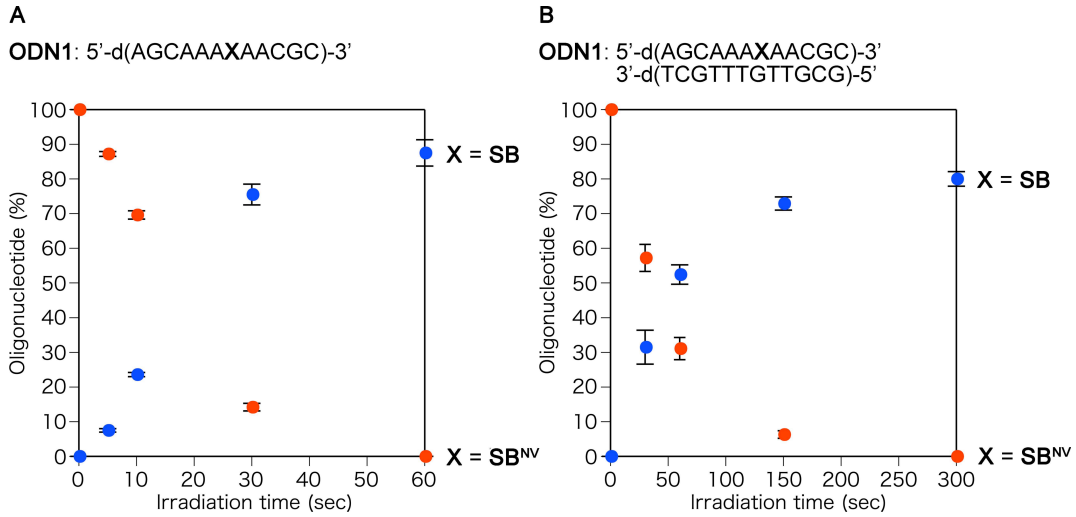

Fig. S2. Time course of the photoreaction (37 ˚C) of (A) **ODN1** and (B) **ODN1** with complementary DNA. Error bars indicate standard deviation (*n* = 3).

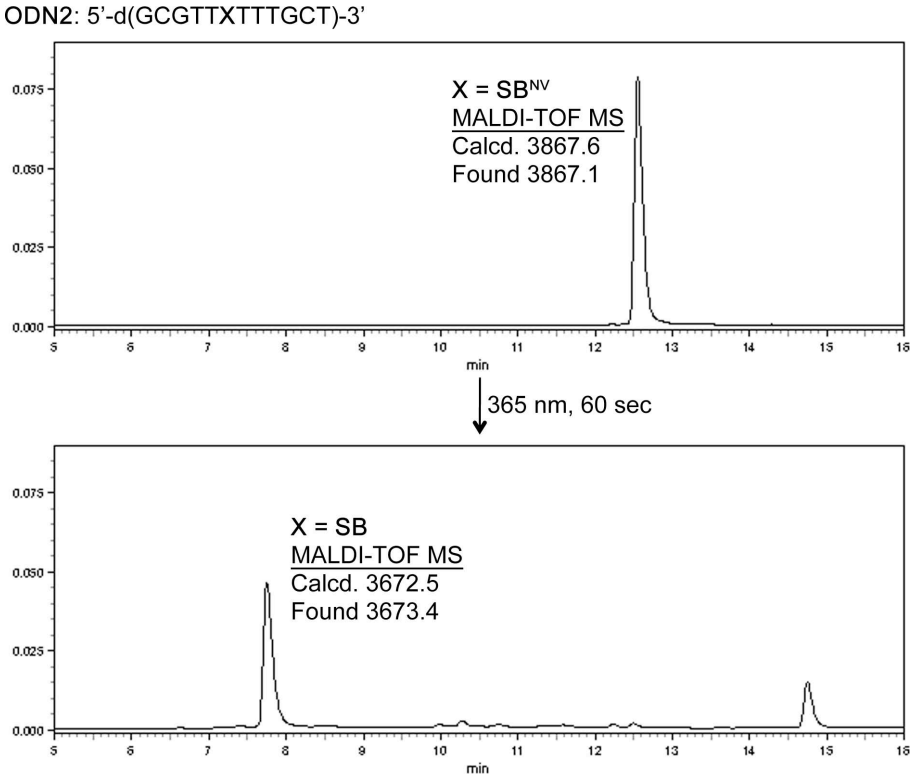

Fig. S3. HPLC analysis of photoreaction of **ODN2**.

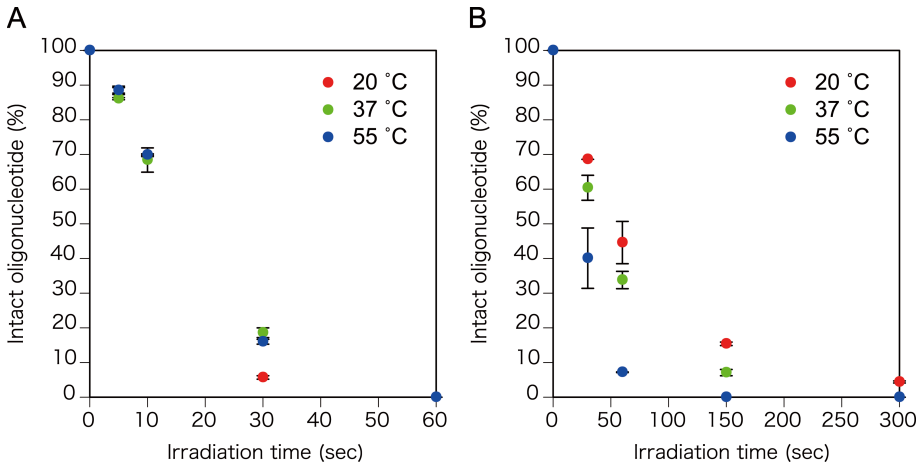

Fig. S4. Influence of the reaction temperature on the efficiency of the photoreaction. (A) **ODN1** (B) **ODN1** with complementary DNA. Error bars indicate standard deviation (*n* = 3).

5. UV melting experiments

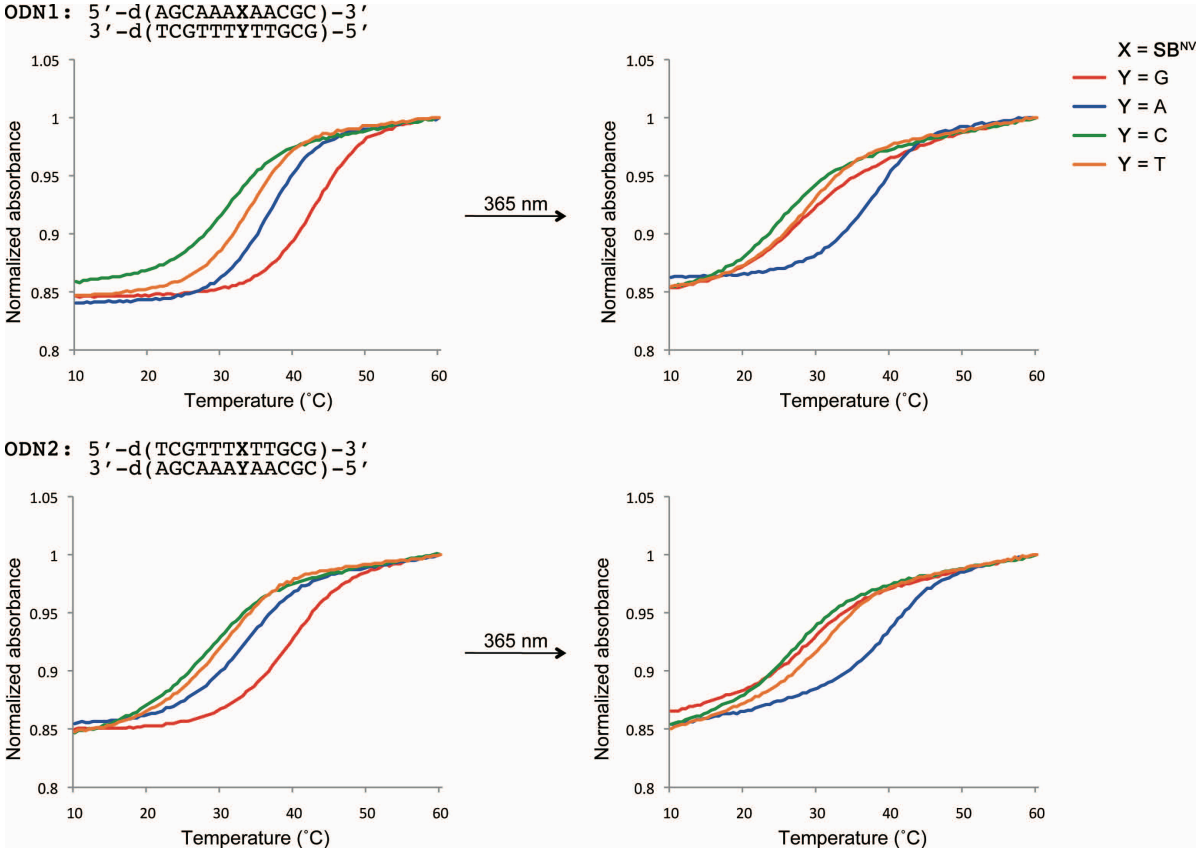

Fig. S5. Changes in UV melting curves for the duplexes with DNA targets triggered by light.

Table S1. Melting temperatures of duplex between **ODN1** and RNA targets

ODN1: 5′-d(AGCAAAXAACGC)-3′
3′-r(UCGUUUYUUGCG)-5′

	T_m (˚C)	
X:Y	-UV	+UV
SB^{NV}:G	25	16
SB^{NV}:A	19	25
SB^{NV}:C	ND	ND
SB^{NV}:U	ND	16
A:U	19	19
G:C	31	31

Table S2. Melting temperatures of duplex between **ODN2** and RNA targets

ODN2: 5′-d(GCGTTXTTTGCT)-3′
3′-r(CGCAAYAAACGA)-5′

	T_m (˚C)	
X:Y	-UV	+UV
SB^{NV}:G	36	32
SB^{NV}:A	30	40
SB^{NV}:C	26	29
SB^{NV}:U	28	32
T:A	40	40
C:G	46	46

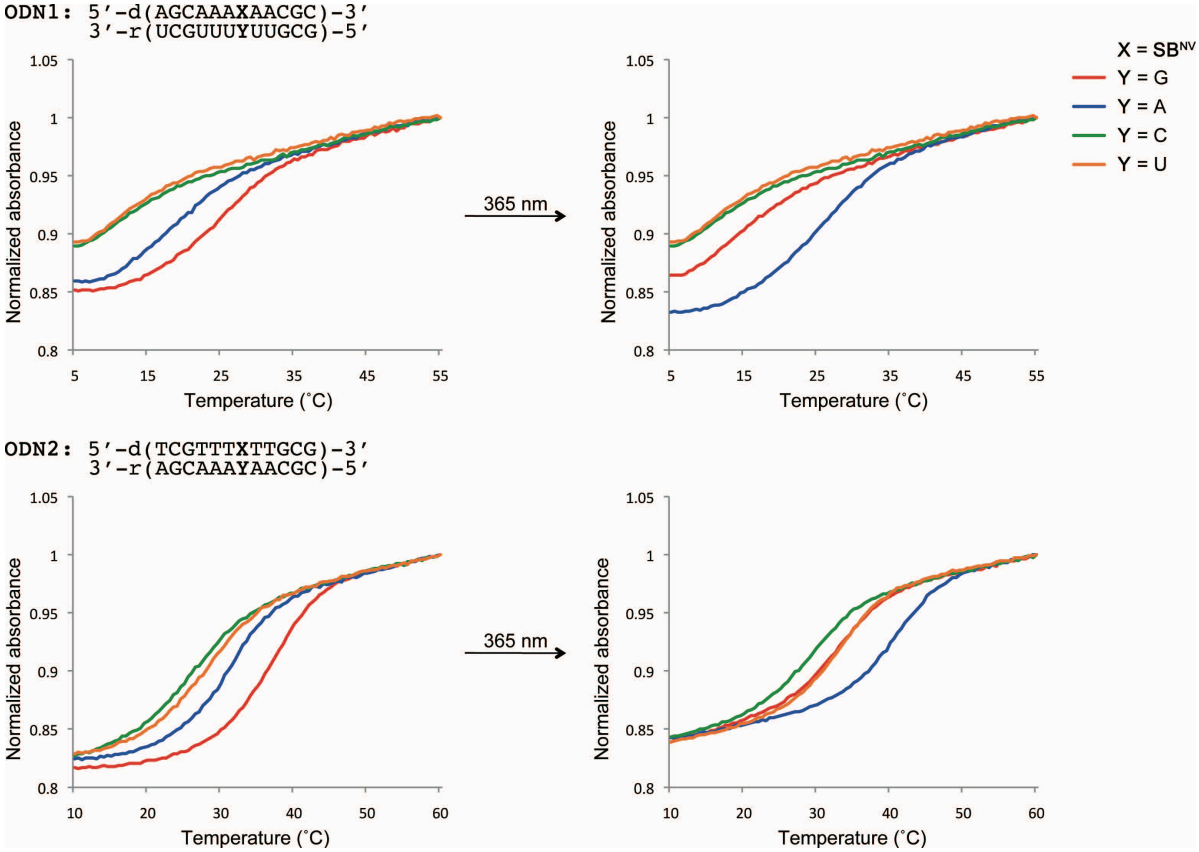

Fig. S6. Changes in UV melting curves for the duplexes with RNA targets triggered by light.

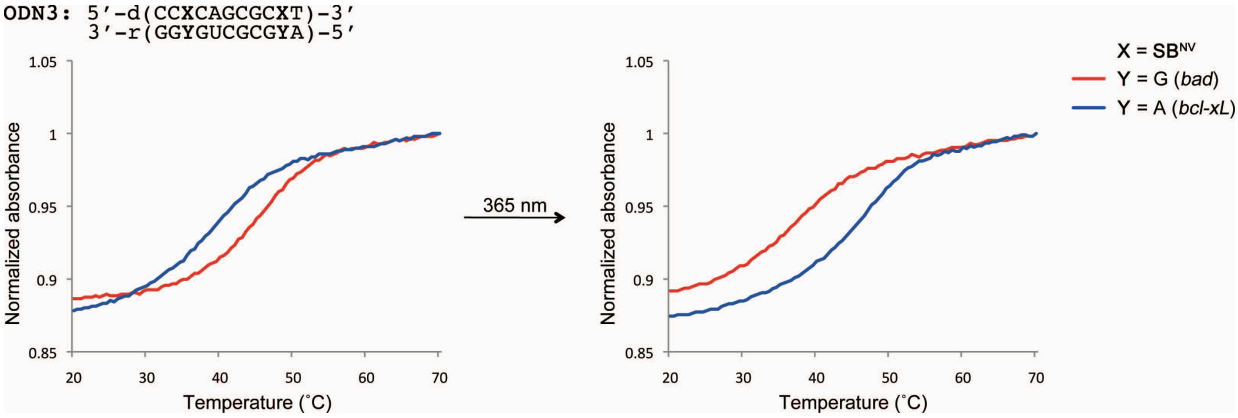

Fig. S7. Changes in UV melting curves for the duplexes **ODN3**/*bad* and **ODN3**/*bcl-xL* triggered by light.

6. Direct observation of light-triggered strand exchange reaction using fluorescent changes

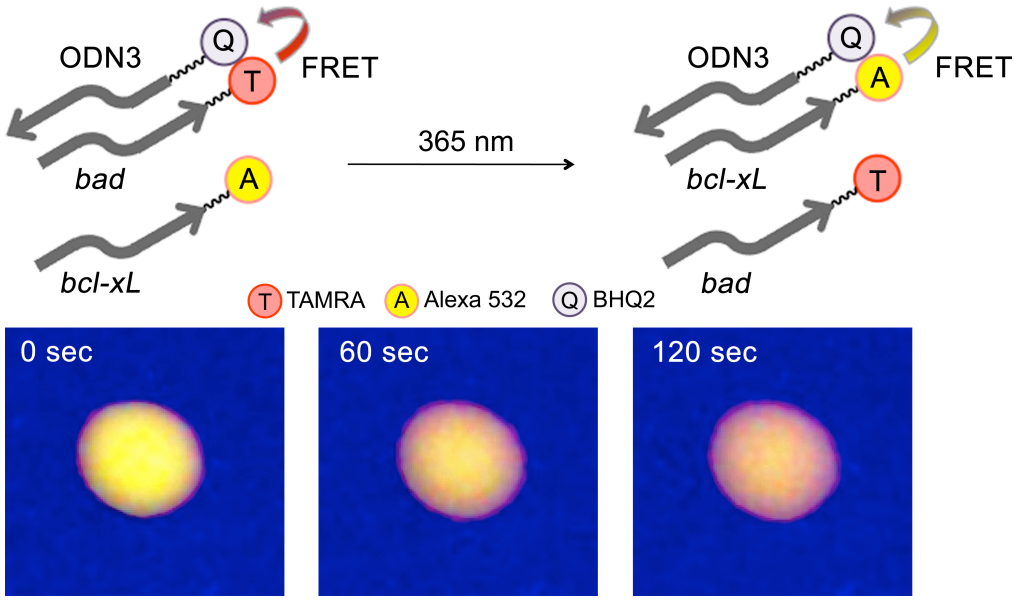

Fig. S8. The fluorescence changes of a liquid drop containing **ODN3**-BHQ2, *bad* and *bcl-xL* upon photoirradiation. Conditions: **ODN3**-BHQ2 (12 μM), *bad* (8 μM), *bcl-xL* (8 μM), NaCl (20 mM), sodium phosphate buffer (10 mM, pH 7.2). Irradiation (365 nm) was performed at room temperature. The fluorescence was observed on a UV transilluminator.